International Journal of Engineering and Technology Innovation, vol. 12, no. 4, 2022, pp. 322-335

Electronically Controlled Biquadratic Filter and Quadrature Oscillator Using CDTAs

Saksit Summart[1,*], Supawadee Sirithai[1], Bongkan Vaisopha[1], Adirek Jantakun[2]

[1]Faculty of Technical Education, Rajamangala University of Technology Isan, Khon Kaen Campus, Khon Kaen, Thailand

[2]Faculty of Engineering, Rajamangala University of Technology Isan, Khon Kaen Campus, Khon Kaen, Thailand

Received 08 August 2021; received in revised form 22 April 2022; accepted 23 April 2022

DOI: https://doi.org/10.46604/ijeti.2022.8230

Abstract

This article presents a current-mode biquadratic filter and quadrature oscillator circuit based on current differencing transconductance amplifiers (CDTAs). The proposed circuit does not require changing the circuit topology. In addition to the low-pass filter, high-pass filter, band-pass filter, and sinusoidal quadrature signal, the proposed circuit has a pole frequency that can be controlled independently from the quality factor, while the oscillation frequency can be controlled non-interactively. The circuit impedance with high output can directly drive the load without using a current buffer. Furthermore, grounded capacitors can function without the use of external resistors. This qualification is ideal for the future development of integrated circuits (ICs). After the PSPICE simulation with 90 nm CMOS parameters and the experiments by commercial ICs, the results are consistent with the theoretical analysis of the proposed circuit.

Keywords: current-mode, quadrature oscillator, biquadratic filter, independent control, CDTA

1. Introduction

Filter and oscillator circuits are essential in electrical and electronic engineering; they are widely used in various measuring instruments, control systems, and signal processing. One such circuit is the biquadratic filter, which can provide necessary qualifications for many communication systems, including phase-locked loop circuits and stereo frequency modulation demodulators. Furthermore, it can be implemented in crossover networks with three-way high-fidelity loudspeakers [1]. Meanwhile, the quadrature oscillator (QO) is an oscillator circuit that produces two sinusoidal signals with a 90-degree phase difference at the same frequency. In telecommunications, quadrature signals are used in single-sideband modulators and quadrature mixers [2]. Many studies from the past decade recommend using a current-mode (CM) active-building block (ABB) as a CM technique to design circuits. The CM technique can provide an extensive dynamic range, inherently wide bandwidth, high slew rate, outstanding linearity, and low power consumption in a circuit [3].

Additionally, many of the CM biquadratic filters and QO using functional building blocks have been present in circuit design. Therefore, many functional building blocks are developed and introduced, which assist in circuit design and reduce the number of passive devices used in the process. For example, the proposed building blocks have parasitic resistances at input terminals and an increasing number of input and output terminals. According to recent research, a CM QO, which is designed using the building block with the most required qualification for the circuit design, can adjust oscillation conditions (OC) independently from the oscillation frequency (OF) and does not require any additional external resistors and floating

* Corresponding author. E-mail address: saksit.su@rmuti.ac.th

Tel.: +668-3-3726340

passive elements. Furthermore, it employs grounded capacitors with high output impedance and can be electronically controlled. Moreover, orthogonally, the quality factor from the pole frequency must be controlled by the CM biquadratic filters circuit [4].

To design a CM QO circuit, the OC and OF must be non-interactively dual-current controlled [5]. However, the lashing circuits are only qualified for biquadratic filters or QOs, with both qualified within the same circuit. Previous studies have presented CM biquadratic filters and QO circuits using building blocks in various ways [4-8]. The designed circuits have demonstrated functional characteristics, with both the biquadratic filter and QO implemented within a single circuit topology. Nevertheless, flaws have been discovered with the proposed circuits. For example, in a CM circuit, the output impedance is insufficient for cascade connection [6], the quality factor cannot be controlled orthogonally from the pole frequency [8], and the proposed circuits are not non-interactively dual-current controlled for both the OC and OF [6-8].

In this study, a CM biquadratic filter and QO circuit is presented without changing the topology. The first model of the proposed circuit can provide transfer functions, which are high-pass (HP), low-pass (LP), and band-pass (BP). The circuit's second function can generate a CM sinusoidal QO when there is no input current under appropriate conditions. Other than that, the pole frequency can also be controlled orthogonally from the quality factor. Similarly, an electronic method can adjust the OC, OF, and non-interactive dual-current control for both the OC and OF. Furthermore, the biquadratic filter and QO can be implemented into integrated circuits (ICs) without additional external resistors and grounded capacitors [9]. Additionally, the proposed circuits are suitable for cascade connection applications in the CM technique, which can directly drive a load due to its high output impedance. Four current differencing transconductance amplifiers (CDTAs) and two grounded capacitors are used in the proposed circuit. The PSPICE simulation program's results are consistent with the theoretical analysis and experiment.

2. Basic Concept of CDTA

CDTA was presented in 2003 as a functional building block for a class of analog signal processing [10]. It is used in both voltage and current modes, including filters and oscillators. The following hybrid matrix represents the characteristics of an ideal CDTA.

$$\begin{bmatrix} v_p \\ v_n \\ i_z \\ i_x \end{bmatrix} = \begin{bmatrix} 0 & 0 & 0 & 0 \\ 0 & 0 & 0 & 0 \\ 1 & -1 & 0 & 0 \\ 0 & 0 & 0 & g_m \end{bmatrix} \begin{bmatrix} i_p \\ i_n \\ v_x \\ v_z \end{bmatrix} \tag{1}$$

The z and x terminals are the output terminals of the CDTA. The z-copy (z_c) is the extended z terminal by utilizing the current mirrors [23]. For complementary metal-oxide semiconductor (CMOS) CDTA, g_m is the transconductance gain expressed in Eq. (2), which can be controlled electronically by the bias current I_B (g_{m1} is the transconductance gain CDTA1). The symbol and equivalent circuit of the CDTA are illustrated in Fig. 1 and Fig. 2, respectively. Fig. 3 shows the CMOS construction used in the simulation of CDTA [24].

$$g_m = \sqrt{kI_B} \tag{2}$$

$$k = \mu_n C_{ox} \left(\frac{W}{L} \right)_{11,12} \tag{3}$$

In Eq. (3), $k = \mu_n C_{ox}(W/L)$ is the physical parameter, μ_n is the carrier mobility, C_{ox} is the gate-oxide capacitance per unit area, and W and L are the effective channel width and length of a CMOS transistor, respectively.

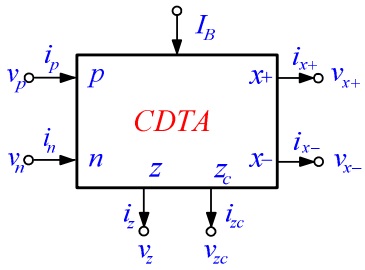

Fig. 1 Symbol of CDTA

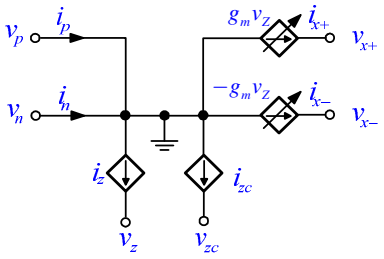

Fig. 2 Equivalent circuit of CDTA

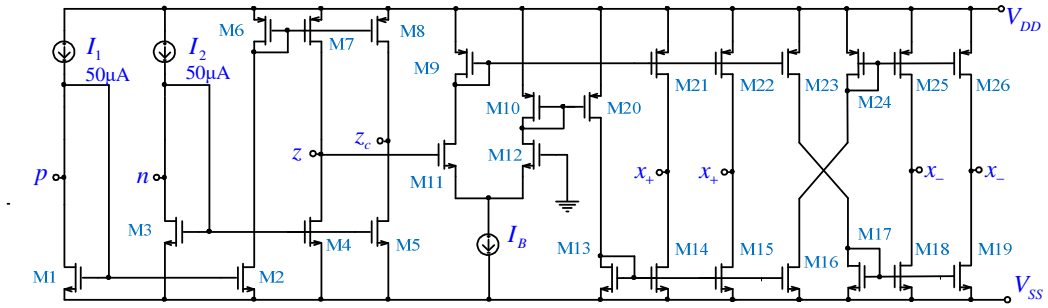

Fig. 3 Internal construction of CDTA

3. Proposed Current-Mode Biquadratic Filter

Fig. 4 depicts the proposed CM biquadratic filter circuit using CDTAs. The circuit uses four CDTAs and two grounded capacitors, without external resistors. The input current flows through a low input impedance (p and n ports), and the output currents are applied at high output impedances at the z and x terminals, allowing the CM circuit to cascade without using a buffer circuit. The output functions of the filter are LP, HP, and BP. The proposed circuit's current transfer functions are as follows:

$$\frac{I_{LP}}{I_{in}} = \frac{-\frac{g_{m1}g_{m2}}{C_1C_2}}{s^2 + \left(\frac{g_{m4}-g_{m3}}{g_{m4}C_1}\right)g_{m1}s + \frac{g_{m1}g_{m2}}{C_1C_2}} \tag{4}$$

$$\frac{I_{HP}}{I_{in}} = \frac{s^2}{s^2 + \left(\frac{g_{m4}-g_{m3}}{g_{m4}C_1}\right)g_{m1}s + \frac{g_{m1}g_{m2}}{C_1C_2}} \tag{5}$$

$$\frac{I_{BP}}{I_{in}} = \frac{\frac{g_{m1}}{C_1}s}{s^2 + \left(\frac{g_{m4}-g_{m3}}{g_{m4}C_1}\right)g_{m1}s + \frac{g_{m1}g_{m2}}{C_1C_2}} \tag{6}$$

From Eqs. (4) to (6), the pole frequency (ω_p), quality factor (Q_p), and bandwidth (BW) can be expressed as:

$$\omega_p = \sqrt{\frac{g_{m1}g_{m2}}{C_1C_2}} \tag{7}$$

$$Q_p = \frac{g_{m4}}{g_{m4}-g_{m3}}\sqrt{\frac{g_{m2}C_1}{g_{m1}C_2}} \tag{8}$$

$$BW = \frac{g_{m1}g_{m4}-g_{m1}g_{m3}}{g_{m4}C_1} \tag{9}$$

Substituting the transconductance as depicted in Eq. (2), the pole frequency and quality factor can be written as:

$$\omega_p = \sqrt{\frac{k\left(I_{B1}I_{B2}\right)^{\frac{1}{2}}}{C_1C_2}} \tag{10}$$

$$Q_p = \frac{\sqrt{I_{B4}}}{\sqrt{I_{B4}}-\sqrt{I_{B3}}}\sqrt{\left(\frac{I_{B2}}{I_{B1}}\right)^{\frac{1}{2}}\left(\frac{C_1}{C_2}\right)} \tag{11}$$

From Eqs. (10) and (11), it is found that the pole frequency can be adjusted by varying I_{B1} and I_{B2}, while the quality factor can be adjusted by I_{B3} or I_{B4}. The pole frequency and quality factor can be adjusted and controlled independently. From Eq. (11), a high-quality factor circuit can set I_{B3} close to I_{B4}. Thus, the bandwidth is given by:

$$BW = \frac{\sqrt{kI_{B1}}}{C_1}\left(\frac{\sqrt{I_{B4}}-\sqrt{I_{B3}}}{\sqrt{I_{B4}}}\right) \tag{12}$$

The sensitivities of the proposed universal biquadratic filter circuit can be shown as:

$$S_{I_{B1}}^{\omega_0} = S_{I_{B2}}^{\omega_0} = S_{I_{B2}}^{Q_0} = \frac{1}{4} \tag{13}$$

$$S_{I_{B1}}^{Q_0} = -\frac{1}{4} \tag{14}$$

$$S_k^{\omega_0} = S_{C_1}^{Q_0} = \frac{1}{2} \tag{15}$$

$$S_{C_2}^{\omega_0} = S_{C_2}^{Q_0} = -\frac{1}{2} \tag{16}$$

$$S_{I_{B3}}^{Q_0} = \frac{1}{4}\frac{\sqrt{I_{B3}}}{\left(\sqrt{I_{B4}}-\sqrt{I_{B3}}\right)^{\frac{1}{2}}} \tag{17}$$

$$S_{I_{B4}}^{Q_0} = \frac{1}{2}\frac{\sqrt{I_{B3}I_{B4}}+I_{B3}}{I_{B4}-2\sqrt{I_{B3}I_{B4}}+I_{B3}} \tag{18}$$

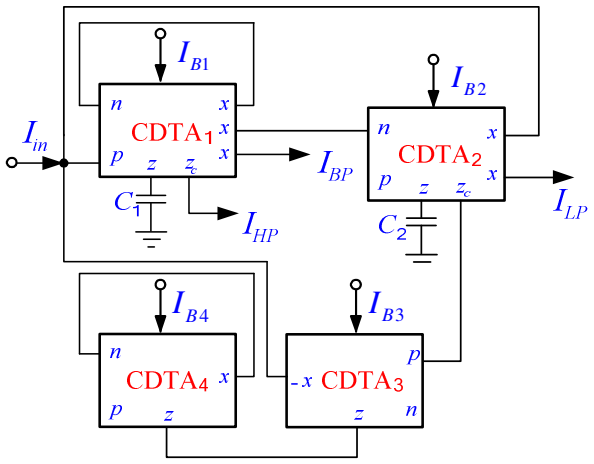

Fig. 4 Proposed CM biquadratic filter

4. Proposed Current-Mode Quadrature Oscillator

According to the proposed biquadratic filter, the proposed circuit can provide CM sinusoidal quadrature signals without an input current under appropriate conditions (Fig. 4). Fig. 5 depicts the proposed CM QO circuit. Additionally, the proposed QO can be compared with previously published QOs based on CDTAs (Table 1) [8, 11-28]. The proposed circuit's characteristic equation is presented as:

$$s^2 + \left(\frac{g_{m4} - g_{m3}}{g_{m4}C_1}\right) g_{m1} s + \frac{g_{m1}g_{m2}}{C_1C_2} = 0 \tag{19}$$

From Eq. (19), the OC and OF are as follows:

$$g_{m4} = g_{m3} \tag{20}$$

$$\omega_{osc} = \sqrt{\frac{g_{m1}g_{m2}}{C_1C_2}} \tag{21}$$

Substituting the transconductance as presented in Eq. (2), the OC and OF are re-written as:

$$I_{B4} = I_{B3} \tag{22}$$

$$\omega_{osc} = \sqrt{\frac{k\left(I_{B1}I_{B2}\right)^{\frac{1}{2}}}{C_1C_2}} \tag{23}$$

From Eqs. (22) and (23), it is found that the OC can be adjusted independently from the OF by varying I_{B3} and I_{B4}, while I_{B1} and I_{B2} can adjust the oscillation frequency without disturbing the OC. Moreover, it should also be noted that the proposed circuit enables non-interactive dual-current control of both the OC and OF. From the circuit in Fig. 5, the current transfer functions of I_{o1} and I_{o2} are:

$$\frac{I_{o2}(s)}{I_{o1}(s)} = -\frac{g_{m2}}{sC_2} \tag{24}$$

For a sinusoidal steady state, Eq. (24) becomes:

$$\frac{I_{o2}(j\omega)}{I_{o1}(j\omega)} = \frac{jg_{m2}}{\omega_{osc}C_2} = \frac{e^{j90^\circ}}{\omega_{osc}C_2} \tag{25}$$

From Eq. (25), the phase difference (θ) between I_{o1} and I_{o2} can be re-written as:

$$\theta = 90^\circ \tag{26}$$

According to Eq. (26), the circuit can provide two sinusoidal current signals with a 90° phase difference and high output impedances that efficiently drive external load without loading effect. The sensitivity of the oscillator circuit is shown in Eqs. (27) to (29).

$$S_{I_{B1}}^{\omega_0} = S_{I_{B2}}^{\omega_0} = \frac{1}{4} \tag{27}$$

$$S_k^{\omega_0} = \frac{1}{2} \tag{28}$$

$$S_{C_1}^{\omega_0} = S_{C_2}^{\omega_0} = -\frac{1}{2} \tag{29}$$

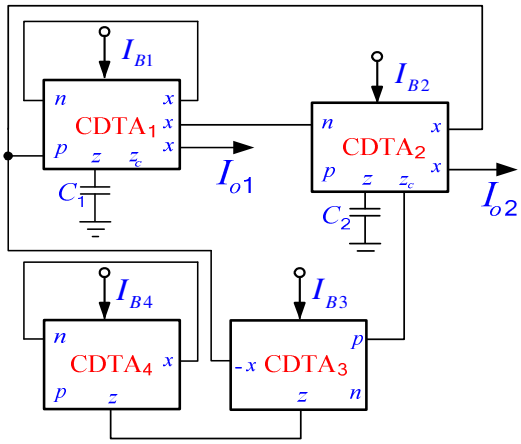

Fig. 5 Proposed CM QO

Table 1 Comparison between various oscillators based on CDTAs

Ref.	Active element	Number of the active element	Number of resistor + capacitor	Grounded capacitor	Non-interactive control for OC and OF	Electronic tune of OC and OF	CM QO
8	CDTA	3	0 + 2	Yes	No	Yes	Yes
11	CDTA	3	0 + 3	Yes	No	Yes	Yes
12	CDTA	3	0 + 3	Yes	No	Yes	Yes
13	CDTA	2	4 + 2	No	No	No	Yes
14	CDTA	2	1 + 2	Yes	No	No	Yes
15	CDTA	2	4 + 2	No	No	No	Yes
16	CDTA	3	0 + 2	Yes	No	Yes	Yes
17	CDTA	3	0 + 2	Yes	No	Yes	Yes
18	CDTA	1	2 + 2	No	No	No	No
19	CDTA	1	1 + 2	No	No	No	Yes
20	CDTA	1	2 + 2	Yes	No	No	No
21	CDTA	2	1 + 2	Yes	No	No	Yes
22	CDTA	1	1 + 2	Yes	No	No	Yes
23	CDTA	4	0 + 2	Yes	No	Yes	Yes
24	CDTA	3	1 + 2	No	No	No	Yes
25	CDTA	2	1 + 2	Yes	No	No	Yes
26	CDTA	3	0 + 2	No	No	Yes	Yes
27	CDTA	2	0 + 2	Yes	No	Yes	Yes
28	CDTA	3	0 + 2	Yes	No	Yes	Yes
Proposed QO	CDTA	4	0 + 2	Yes	Yes	Yes	Yes

5. Analysis of Current Tracking Error

For the non-ideal case, the transconductance gain error of CDTA is used to prove the proposed circuit's performance. It has a significant effect on current and voltage gain errors. In Eq. (1), CDTA's characteristic equation can be expressed as:

$$\begin{bmatrix} v_p \\ v_n \\ i_z \\ i_x \end{bmatrix} = \begin{bmatrix} 0 & 0 & 0 & 0 \\ 0 & 0 & 0 & 0 \\ \alpha_p & -\alpha_n & 0 & 0 \\ 0 & 0 & 0 & \beta g_m \end{bmatrix} \begin{bmatrix} i_p \\ i_n \\ v_x \\ v_z \end{bmatrix} \tag{30}$$

The parameters beta (β) and alpha (α) are the voltage and current transfer gain errors deviating from one, depending on the value of intrinsic impedances and temperatures. These errors affect the proposed circuit's temperature sensitivity and high-frequency response, so the CDTA should be carefully designed to minimize these errors. In light of this, these deviations are minor and can be overlooked in the theory. In the non-ideal case, the universal filter's current transferring functions from Eqs. (4) to (6) become:

$$\frac{I_{LP}}{I_{in}} = \frac{-\frac{\alpha_{p1}\alpha_{n2}\beta_1\beta_2 g_{m1}g_{m2}}{C_1C_2}}{F(s)} \tag{31}$$

$$\frac{I_{HP}}{I_{in}} = \frac{\alpha_{p1}s^2}{F(S)} \tag{32}$$

$$\frac{I_{BP}}{I_{in}} = \frac{\frac{\alpha_{p1}\beta_1 g_{m1}}{C_1}s}{F(s)} \tag{33}$$

where

$$F(s) = \begin{Bmatrix} s^2 + \left(\frac{\alpha_{n1}\alpha_{n4}\beta_4 g_{m4} - \alpha_{p1}\alpha_{n2}\alpha_{p3}\beta_3 g_{m3}}{\alpha_{n4}\beta_4 g_{m4}C_1}\right) \\ \beta_1 g_{m1}s + \frac{\alpha_{p1}\alpha_{n2}\beta_1\beta_2 g_{m1}g_{m2}}{C_1C_2} \end{Bmatrix} \tag{34}$$

In this case, the pole frequency, quality factor, and bandwidth in Eqs. (7) to (9) are changed to:

$$\omega_p = \sqrt{\frac{\alpha_{p1}\alpha_{n2}\beta_1\beta_2 g_{m1}g_{m2}}{C_1C_2}} \tag{35}$$

$$Q_p = \begin{Bmatrix} \frac{\alpha_{n4}\beta_4 g_{m4}}{\alpha_{n1}\alpha_{n4}g_{m4}\beta_4 - \alpha_{p1}\alpha_{n2}\alpha_{p3}\beta_3 g_{m3}} \\ \sqrt{\frac{\alpha_{p1}\alpha_{n2}\beta_2 g_{m2}C_1}{g_{m1}\beta_1 C_2}} \end{Bmatrix} \tag{36}$$

$$BW = \beta_1 g_{m1}\frac{\alpha_{n1}\alpha_{n4}g_{m4}\beta_4 - \alpha_{p1}\alpha_{n2}\alpha_{p3}\beta_3 g_{m3}}{\alpha_{n4}\beta_4 g_{m4}} \tag{37}$$

In the non-ideal case, the CM QO, characteristic equation, OC, and OF from Eqs. (19) to (21) are expressed as follows:

$$\begin{Bmatrix} s^2 + \left(\frac{\alpha_{n1}\alpha_{n4}\beta_4 g_{m4} - \alpha_{p1}\alpha_{n2}\alpha_{p3}\beta_3 g_{m3}}{\alpha_{n4}\beta_4 g_{m4}C_1}\right) \\ \beta_1 g_{m1}s + \frac{\alpha_{p1}\alpha_{n2}\beta_1\beta_2 g_{m1}g_{m2}}{C_1C_2} \end{Bmatrix} = 0 \tag{38}$$

$$\alpha_{n1}\alpha_{n4}\beta_1\beta_4 g_{m4} = \alpha_{p1}\alpha_{n2}\alpha_{p3}\beta_1\beta_3 g_{m3} \tag{39}$$

$$\omega_{osc} = \sqrt{\frac{\alpha_{p1}\alpha_{n2}\beta_1\beta_2 g_{m1}g_{m2}}{C_1C_2}} \tag{40}$$

6. Analysis of Parasitic Resistance and Capacitance

The R_p and R_n are the parasitic resistances of p and n at the input terminals, respectively. In addition, the output z and x terminals consist of parasitic resistances and capacitances (R_z, C_z, R_x, and C_x) from terminals z and x to the ground. The parasitic capacitances and resistances of CDTA are presented in Fig. 6. If the parasitic resistances at the z and x terminals are much greater than the parasitic resistance at the p and n terminals (R_x, $R_z >> R_p$, R_n), for the CM biquadratic filter and QO, the transfer function of the proposed circuits is:

$$D(s)=\begin{Bmatrix}(C_1+C_{Z1})(C_{z3}+C_{z4})(C_2+C_{Z2})s^3+(C_2+C_{Z2})[g_{m4}(C_1+C_{Z1})+g_{m1}(C_{z3}+C_{z4})]s^2\\+[g_{m1}g_{m4}(C_2+C_{Z2})+g_{m1}g_{m2}(C_{z3}+C_{z4})-g_{m1}g_{m3}(C_2+C_{Z2})]s+g_{m1}g_{m2}g_{m4}\end{Bmatrix} \tag{41}$$

For the CM biquadratic filter, the transfer function with general third-order transfer functions is given by:

$$D(s)=s^3+\omega_p\left(1+\frac{1}{Q_p}\right)s^2+\omega_o^2\left(1+\frac{1}{Q_p}\right)s+\omega_p^3 \tag{42}$$

By comparing Eq. (41) with Eq. (42), it will get:

$$\omega_p^3=\frac{g_{m1}g_{m2}g_{m4}}{C'C''C'''} \tag{43}$$

$$\omega_p^2\left(1+\frac{1}{Q_p}\right)=\frac{g_{m1}g_{m4}C''+g_{m1}g_{m2}C'''-g_{m1}g_{m3}C''}{C'C''C'''} \tag{44}$$

$$\omega_p\left(1+\frac{1}{Q_p}\right)=\frac{C''(g_{m4}C'+g_{m1}C''')}{C'C''C'''} \tag{45}$$

where $C'=C_1+C_{Z1}$, $C''=C_2+C_{Z2}$, and $C'''=C_{Z3}+C_{Z4}$.

In this case, the pole frequency, quality factor, and bandwidth in Eqs. (7) to (9) are changed to:

$$\omega_p=\sqrt[3]{\frac{g_{m1}g_{m2}g_{m4}}{C'C''C'''}} \tag{46}$$

$$Q_p=\frac{1}{\frac{C''(g_{m4}C'+g_{m1}C''')}{\omega_pC'C''C'''}-1} \tag{47}$$

$$BW=\frac{C''(g_{m4}C'+g_{m1}C''')}{C'C''C''}-\omega_p \tag{48}$$

where $C'=C_1+C_{Z1}$, $C''=C_2+C_{Z2}$, and $C'''=C_{Z3}+C_{Z4}$.

Additionally, for the CM QO, the OC and OF from Eqs. (19) to (21) are represented as follows:

$$C'\left(C''\right)^2C'''\left[g_{m4}C'+g_{m1}C'''\right]=g_{m1}^2g_{m2}g_{m4}\left[g_{m4}C''+g_{m2}C'''-g_{m3}C''\right] \tag{49}$$

$$\omega_{osc}=\sqrt{\frac{g_{m1}g_{m2}g_{m4}}{C''(g_{m4}C'+g_{m1}C''')}} \tag{50}$$

where $C'=C_1+C_{Z1}$, $C''=C_2+C_{Z2}$, and $C'''=C_{Z3}+C_{Z4}$.

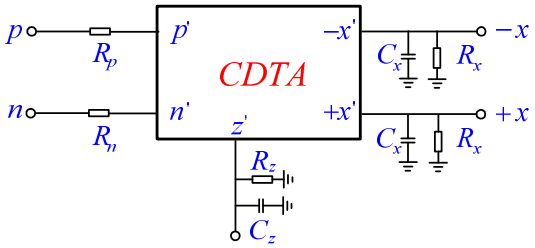

Fig. 6 Parasitic resistances and capacitances of CDTA

7. Simulation and Experimental Results

The PSPICE simulation program is used to substantiate the biquadratic filter's theoretical prediction in Fig. 4. The circuit is built with $C_1 = C_2 = 0.5$ pF, $I_{in} = 1$ µA, $I_{B1} = I_{B2} = I_{B4} = 100$ µA, and $I_{B3} = 50$ µA. With these component values, the pole frequency can be adjusted without affecting the quality factor, as analyzed in Eqs. (10) and (11), respectively, where the calculated value of pole frequency yields 930.783 MHz. The CMOS implementation of the internal construction of CDTA used in the simulation is presented in Fig. 3. The 90 nm EKV MOSFET Model (EKV v301.01) of EPFL technology is used in the internal construction of CDTA [29]. The ratio of dimensions of the p-type metal-oxide semiconductor (PMOS) and n-type metal-oxide semiconductor (NMOS) are presented in Table 2. The circuit is biased with ±1.2 V supply voltages and the simulation results of pole frequency are 903.650 MHz. The pole frequency deviated from Eq. (10) is about 2.915%. This deviation may occur with the voltage and current tracking errors of CDTAs. In this case, the value changes because the CMOS implementation used in the circuit deviates from the non-ideal properties and the effect of parasitic elements.

Fig. 7 shows the frequency and gain responses of the universal filter obtained from Fig. 4. The circuit allows simultaneous LP, HP, and BP filter responses. Fig. 8 illustrates the BP function by varying bias currents ($I_{B1} = I_{B2}$). Fig. 8(a) shows that the frequency responses at the bias currents are 60 µA, 100 µA, 150 µA, and 200 µA, respectively. In addition, the electronic tune is confirmed by varying bias currents from 60 µA to 260 µA; Fig. 8(b) presents the variation frequency. Fig. 9 presents the frequency responses of the BP function by changing the bias current I_{B3} to be 50 µA, 60 µA, 70 µA, 80 µA, and 90 µA, respectively. This means that the quality factor of the proposed circuit can be adjusted by I_{B3} which is independent of the pole frequency.

Moreover, a sine wave is set with 1 µA at the pole frequency to the input current of the proposed filter circuit. The confirmed BP response (the transient response and the frequency spectrum) is presented in Fig. 10. The total harmonic distortion (THD) at the pole frequency (930.783 MHz) of about 0.089% is presented in Table 3. Additionally, the Monte Carlo simulation is employed to investigate the stability of the proposed filter by using 5% of the tolerances of the capacitance of capacitors and the transconductance parameter of transistors (μC_{ox}). The simulation results are illustrated in Fig. 11.

To verify the theoretical prediction of the proposed QO in Fig. 5, the PSPICE simulation uses $C_1 = C_2 = 0.1$ nF, $I_{B1} = I_{B2} = 100$ µA, $I_{B3} = 50.3$ µA, and $I_{B4} = 50$ µA. The DC supply voltages of the circuit are biased with ±1.2 V. The simulation circuit's OF is 4.6 MHz, whereas the calculated value of this parameter from Eq. (23) is 4.654 MHz, deviating about 1.16%. Fig. 12 shows the simulated quadrature output waveforms in the steady states. The simulated frequency spectrums of output currents are indicated in Fig. 13. The THD values of I_{o1} and I_{o2} are approximately 1.469% and 2.235%, respectively, according to the harmonics distortion analysis results presented in Tables 4 and 5. Tables 4 and 5 indicate that the output currents I_{o1} and I_{o2} have phase differences and total power dissipation of around 90.3 degrees and 5.81 mW, respectively. Fig. 14 shows the electronic tuning of the OF with the bias current $I_{B1} = I_{B2}$ for varying capacitor values.

Furthermore, the proposed oscillator's stability is introduced by the Monte Carlo simulation; the tolerances of capacitances and the transconductance parameters are 5%. Fig. 15 depicts the simulation outcome. In addition, AD844 and LM13700 commercial ICs are used in the experiment. The circuit used ±12 V, $C_1 = C_2 = 0.1$ nF, $I_{B1} = I_{B2} = 300$ µA, $I_{B3} = 85$ µA, and $I_{B4} = 70$ µA. The internal construction of CDTA used in the experiment is presented in Fig. 16. The measurement of

quadrature output waveforms during a steady state is illustrated in Fig. 17. The output voltage of the quadrature signals in time-domain waveforms is a sinusoidal signal with a frequency of 909.120 kHz. The calculated value of this parameter from Eq. (23) is 918.202 kHz, and the frequency deviation from the experiment is 0.441%.

Table 2 Dimensions of CMOS transistors

Transistor	M1-M8	M9	M10-M11	M12	M13-M19	M22-M26
W (nm)	10	5	90	40	90	60
L (nm)	1	1	1	1	1	1

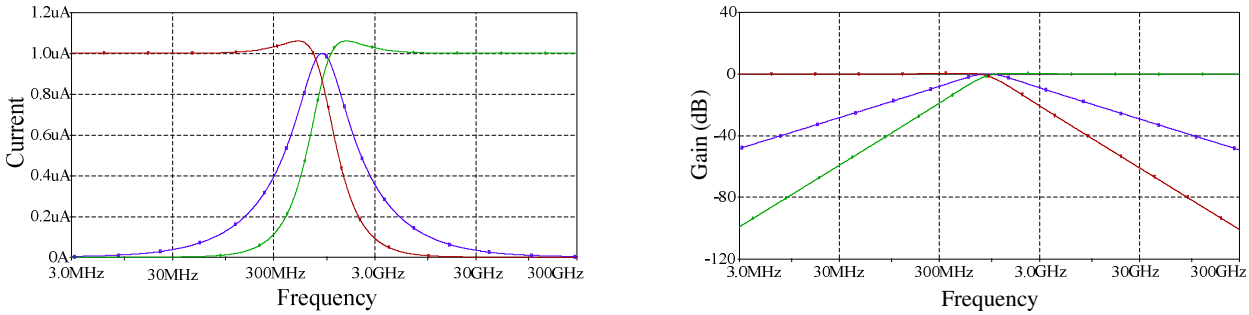

(a) Frequency response (b) Gain response

Fig. 7 Frequency and gain responses of the proposed biquadratic filter

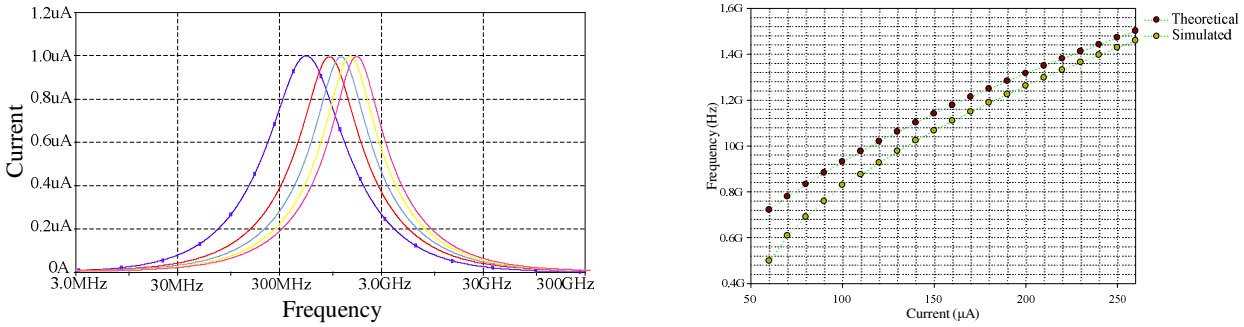

(a) Frequency response (b) Pole frequencies against bias currents for $I_{B1} = I_{B2}$

Fig. 8 Simulation of the BP function for different values of $I_{B1} = I_{B2}$

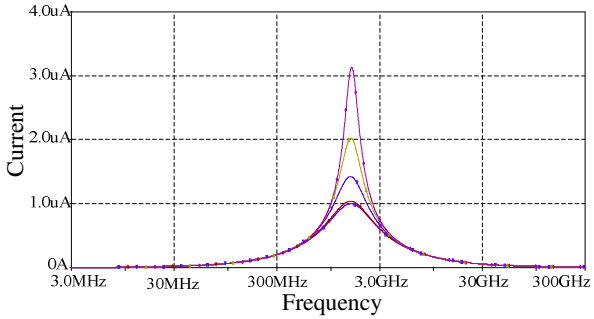

Fig. 9 Frequency response of the BP function for different values of I_{B3}

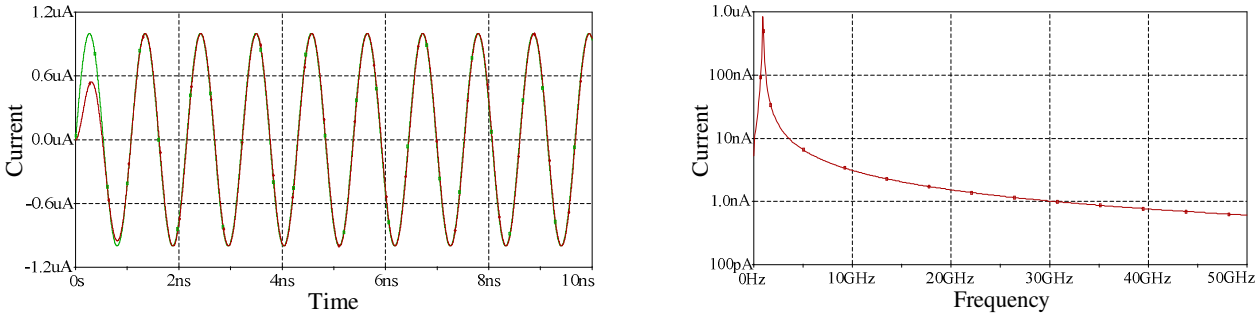

(a) Transient response (b) Frequency spectrum

Fig. 10 Simulation of the BP function at the pole frequency (930.783 MHz)

Table 3 THD of the BP function at the pole frequency (930.783 MHz)

Harmonic no.	Frequency (Hz)	Fourier component (A)	Phase (degree)
1	9.308E+08	9.987E-07	1.078E+02
2	1.862E+09	8.898E-10	2.569E+01
3	2.792E+09	4.208E-11	-1.658E+02
4	3.723E+09	3.312E-11	-1.156E+02
5	4.654E+09	2.446E-11	-7.466E+01
6	5.585E+09	2.178E-11	-2.640E+01
7	6.515E+09	1.485E-11	2.419E+01
8	7.446E+09	1.162E-11	7.890E+01
9	8.377E+09	1.130E-11	1.426E+02
10	9.308E+09	1.040E-11	-1.645E+02
DC component = -5.120588E-11 Total harmonic distortion = 8.935764E-02 percent Total power dissipation = 6.34E-03 Watts			

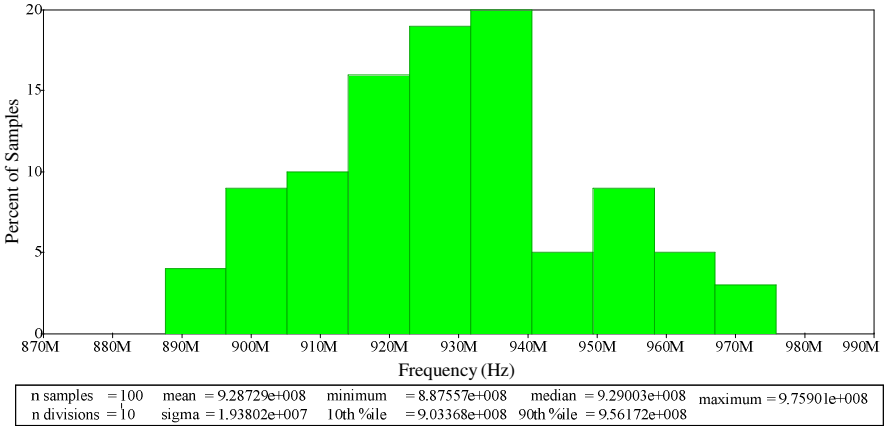

Fig. 11 Monte Carlo simulation of the biquadratic filter

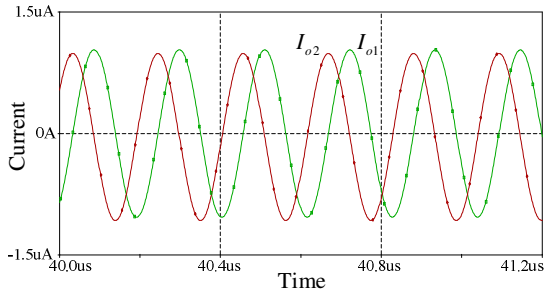

Fig. 12 Simulation result of output waveforms in the steady state

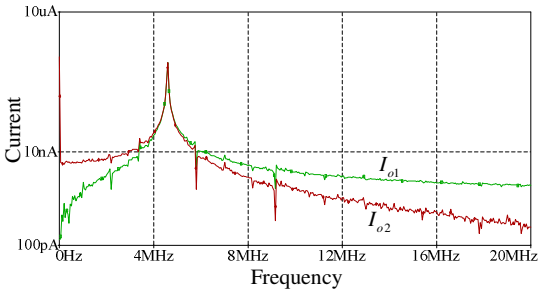

Fig. 13 Simulation result of the output spectrum

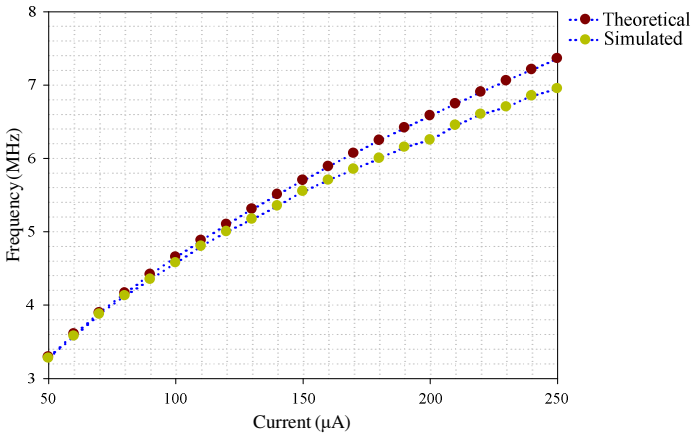

Fig. 14 Oscillation frequencies against bias currents for $I_{B1} = I_{B2}$

Table 4 THD of I_{o1}

Harmonic no.	Frequency (Hz)	Fourier component (A)	Phase (degree)
1	4.600E+06	9.639E-07	1.412E+02
2	9.200E+06	7.738E-09	1.106E+02
3	1.380E+07	3.612E-09	1.083E+02
4	1.840E+07	3.332E-09	1.060E+02
5	2.300E+07	3.237E-09	1.038E+02
6	2.760E+07	3.131E-09	1.003E+02
7	3.220E+07	3.155E-09	9.479E+01
8	3.680E+07	3.275E-03	8.863E+01
9	4.140E+07	3.608E-03	8.024E+01
10	4.600E+07	8.319E-03	-1.338E+02
DC component = 6.153910E-11 Total harmonic distortion = 1.469477E+00 Percent Total power dissipation = 5.81E-03 Watts			

Table 5 THD of I_{o2}

Harmonic no.	Frequency (Hz)	Fourier component (A)	Phase (degree)
1	4.600E+06	9.652E-07	-1.285E+02
2	9.200E+06	9.424E-09	-1.185E+02
3	1.380E+07	7.164E-09	-1.021E+02
4	1.840E+07	6.560E-09	-1.012E+02
5	2.300E+07	6.417E-09	-1.016E+02
6	2.760E+07	6.252E-09	-1.015E+02
7	3.220E+07	6.114E-09	-9.990E+01
8	3.680E+07	5.748E-09	-9.949E+01
9	4.140E+07	5.852E-09	-9.710E+01
10	4.600E+07	9.871E-09	1.770E+02
DC component = 1.078746E-06 Total harmonic distortion = 2.235400E+00 Percent Total power dissipation = 5.81E-03 Watts			

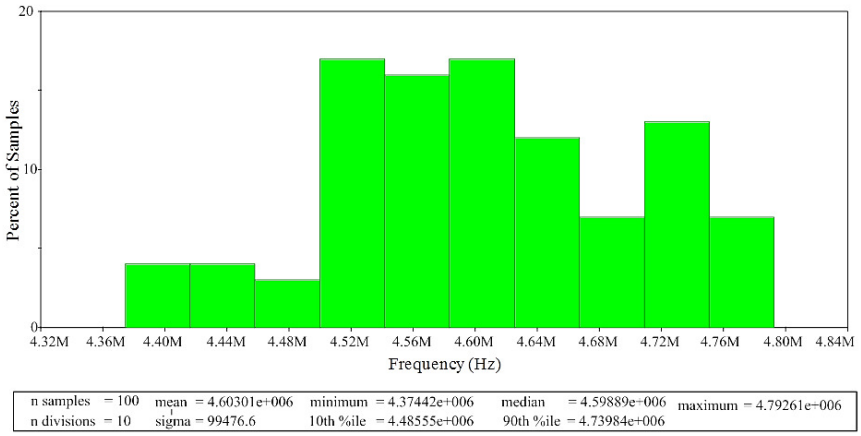

Fig. 15 Monte Carlo simulation of the proposed QO

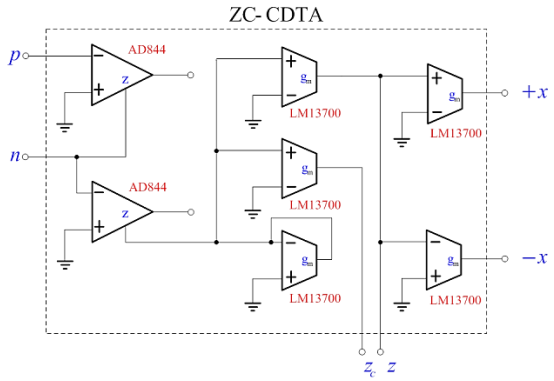

Fig. 16 Implementation of CDTA using commercial ICs

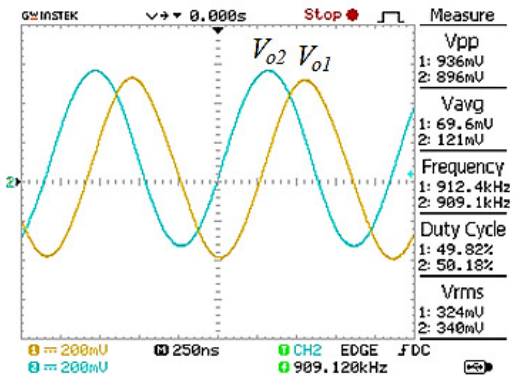

Fig. 17 Measured waveforms of V_{o1} and V_{o2}

8. Conclusions

This study introduced a CM biquadratic filter and QO implemented in the same circuit topology. The CM biquadratic filter can control the pole frequency without affecting the quality factor, and it has three transferring functions. In addition, the OC and OF can be controlled by adjusting bias currents with non-interactively dual-current control. The proposed circuits are ideal for ICs, and it consists of four CDTAs and two grounded capacitors without additional external resistors. Moreover, 90 nm CMOS parameters are used for the internal construction of CMOS transistors for simulation. The proposed circuit can generate high frequency and low power consumption, which is appropriate for the design of ICs [30]. Additionally, the oscillator circuit is demonstrated using commercial ICs such as AD844 and LM13700. The simulation and experiment findings are consistent with the theoretical analysis.

Acknowledgments

This research was supported by the Faculty of Technical Education at Rajamangala University of Technology Isan, Khon Kaen Campus, Khon Kaen, 40000, Thailand.

Conflicts of Interest

The authors declare that they have no conflicts of interest.

References

[1] M. A. Ibrahim, et al., "A 22.5 MHz Current-Mode KHN-Biquad Using Differential Voltage Current Conveyor and Grounded Passive Elements," AEÜ—International Journal of Electronics and Communications, vol. 59, no. 5, pp. 311-318, July 2005.

[2] I. A. Khan, et al., "An Integrable gm-C Quadrature Oscillator," International Journal of Electronics, vol. 87, no. 11, pp. 1353-1357, November 2000.

[3] U. Çam, et al., "Current-Mode High Output-Impedance Sinusoidal Oscillator Configuration Employing Single FTFN," Analog Integrated Circuits and Signal Processing, vol. 24, no. 3, pp. 231-238, September 2000.

[4] C. Wang, et al., "A New Current-Mode Current Controlled SIMO-Type Universal Filter," AEÜ—International Journal of Electronics and Communications, vol. 65, no. 3, pp. 231-234, March 2011.

[5] A. Jantakun, "Current-Mode Quadrature Oscillator Using CCCCTAs with Non-Interactive Current Control for CO, FO and Amplitude," Journal of Microelectronics, Electronic Components, and Materials, vol. 45, no.1, pp. 47-56, 2015.

[6] W. Kiranon, et al., "Electronically Tunable Multifunctional Translinear-C Filter and Oscillator," Electronics Letters, vol. 33, no. 7, pp. 573-574, March 1997.

[7] M. Siripruchyanun, et al., "Cascadable Current-Mode Biquad Filter and Quadrature Oscillator Using DO-CCCIIs and OTA," Circuits, Systems, and Signal Processing, vol. 28, no. 1, pp. 99-110, February 2009.

[8] J. Jin, "Current-Mode Resistorless SIMO Universal Filter and Four-Phase Quadrature Oscillator," International Journal of Electrical, Computer, Electronics, and Communication Engineering, vol. 7, pp. 149-154, 2013.

[9] A. M. Soliman, "New Grounded Capacitor Current-Mode Band-Pass Low-Pass Filters Using Two Balanced Output ICCII," Journal of Active and Passive Electronic Devices, vol. 3, pp. 175-184, 2008.

[10] D. Biolek, "CDTA-Building Block for Current-Mode Analog Signal Processing," European Conference on Circuit Theory and Design, pp. 397-400, September 2003.

[11] J. W. Horng, "Current-Mode Third-Order Quadrature Oscillator Using CDTAs," Active and Passive Electronic Components, vol. 2009, Article no. 789171, 2009.

[12] J. W. Horng, et al., "Electronically Tunable Third-Order Quadrature Oscillator Using CDTAs," Radioengineering, vol. 19, no. 2, pp. 326-330, June 2010.

[13] A. U. Keskin, et al., "Current-Mode Quadrature Oscillator Using Current Differencing Transconductance Amplifiers (CDTA)," IEE Proceedings—Circuits, Devices, and System, vol. 153, no. 3, pp. 214-218, July 2005.

[14] A. Lahiri, "New Current-Mode Quadrature Oscillator Using CDTA," IEICE Electronics Express, vol. 6, no. 3, pp. 135-140, February 2009.

[15] A. Uygur, et al., "CDTA-Based Quadrature Oscillator Design," 14th European Signal Processing Conference, pp. 1-4, September 2006.

[16] W. Tangsrirat, et al., "Current-Mode Sinusoidal Quadrature Oscillator with Independent Control of Oscillation Frequency and Condition Using CDTAs," Indian Journal of Pure and Applied Physics, vol. 48, pp. 363-366, May 2010.

[17] W. Tanjaroen, et al., "Resistorless Current-Mode Quadrature Sinusoidal Oscillator Using CDTAs," APSIPA Annual Summit and Conference, pp. 307-310, October 2009.

[18] D. Prasad, et al., "Realisation of Single-Resistance-Controlled Sinusoidal Oscillator: A New Application of the CDTA," WSEAS Transactions on Electronics, vol. 5, no. 6, pp. 257-259, June 2008.

[19] W. Jaikla, et al., "A Simple Current-Mode Quadrature Oscillator Using Single CDTA," Radioengineering, vol. 17, no. 4, pp. 33-40, December 2008.

[20] D. Biolek, et al., "Grounded Capacitor Current Mode Single Resistance-Controlled Oscillator Using Single Modified Current Differencing Transconductance Amplifier," IEE Proceedings—Circuits, Devices, and System, vol. 4, no. 6, pp. 496-502, November 2010.

[21] M. Kumngern, et al., "Electronically Tunable Current-Mode Quadrature Oscillator Using Current Differencing Transconductance Amplifiers," IEEE Region 10 Conference (TENCON 2009), pp. 1-4, December 2009.
[22] T. Bumrongchoke, et al., "Current Differencing Transconductance Amplifier Based Current-Mode Quadrature Oscillator Using Grounded Capacitors," 10th International Symposium on Communications and Information Technologies, pp. 192-195, October 2010.
[23] D. Biolek, et al., "Current Mode Quadrature Oscillator Using Two CDTAs and Two Grounded Capacitors," WSEAS International Conference on System Science and Simulation in Engineering, pp. 368-370, December 2006.
[24] J. Jin, et al., "Current-Mode Four-Phase Quadrature Oscillator Using Current Differencing Transconductance Amplifier Based First-Order Allpass Filter," Revue Roumaine des Sciences Techniques—Série Électrotechnique et Énergétique, vol. 57, no. 3, pp. 291-300, 2012.
[25] A. Lahiri, "Novel Voltage/Current-Mode Quadrature Oscillator Using Current Differencing Transconductance Amplifier," Analog Integrated Circuits and Signal Processing, vol. 61, no. 2, pp. 199-203, March 2009.
[26] W. Tangsrirat, et al., "Resistorless Realization of Current-Mode First-Order Allpass Filter Using Current Differencing Transconductance Amplifiers," Microelectronics Journal, vol. 41, no. 2-3, pp. 178-183, February 2010.
[27] N. Pandey, et al., "Single CDTA-Based Current Mode All-Pass Filter and Its Applications," Journal of Electrical and Computer Engineering, vol. 2011, Article no. 897631, 2011.
[28] S. Summart, et al., "New Current-Controlled Current-Mode Sinusoidal Quadrature Oscillators Using CDTAs," AEÜ—International Journal of Electronics and Communications, vol. 69, no. 1, pp. 62-68, January 2015.
[29] S. Yoshitomi, et al., "EKV3 Parameter Extraction and Characterization of 90 nm RF-CMOS Technology," 14th International Conference on Mixed Design of Integrated Circuits and Systems, pp. 74-79, June 2007.
[30] D. Lakshmaiah, et al., "Theoretical Analysis of CMOS Circuits in 90 nm Technology," International Journal of Innovative Technology and Exploring Engineering, vol. 8, no. 4S2, pp. 368-371, March 2019.